Published in final edited form as:
Neuron. 2014 April 16; 82(2): 380–397. doi:10.1016/j.neuron.2014.02.040.

CSF1 receptor signaling is necessary for microglia viability, which unmasks a cell that rapidly repopulates the microglia-depleted adult brain

Monica Renee Pittman Elmore[1,*], **Allison Rachel Najafi**[1,*], **Maya Allegra Koike**[1], **Nabil Nazih Dagher**[1], **Elizabeth Erin Spangenberg**[1], **Rachel Anne Rice**[1], **Masashi Kitazawa**[3], **Bernice Matusow**[2], **Hoa Nguyen**[2], **Brian Lee West**[2], and **Kim Nicholas Green**[1]

[1]Department of Neurobiology and Behavior, Institute for Memory Impairments and Neurological Disorders, University of California, Irvine, CA 92697-4545

[2]Plexxikon Inc., Berkeley, California

[3]Department of Molecular and Cell Biology, University of California, Merced

Abstract

The colony stimulating factor 1 receptor (CSF1R) is a key regulator of myeloid lineage cells. Genetic loss of the CSF1R blocks the normal population of resident microgliain the brain that originates from the yolk sac during early development. However, the role of CSF1R signaling in microglial homeostasis in the adult brain is largely unknown. To this end, we tested the effects of selective CSF1R inhibitors on microglia in adult mice. Surprisingly, extensive treatment results in elimination of ~99% of all microglia brain-wide, showing that microglia in the adult brain are physiologically dependent upon CSF1R signaling. Mice depleted of microglia show no behavioral or cognitive abnormalities, revealing that microglia are not necessary for these tasks. Finally, we discovered that the microglia-depleted brain completely repopulates with new microglia within one week of inhibitor cessation. Microglial repopulation throughout the CNS occurs through proliferation of nestin positive cells that then differentiate into microglia.

Keywords

microglia; colony-stimulating factor 1 receptor; behavior; inflammation; nestin; progenitor

Address correspondence to: Kim N. Green, Ph.D., 3208 Biological Sciences III, University of California, Irvine, Irvine, CA 92697-4545, Tel: 949 824 3859, kngreen@uci.edu.
*These authors contributed equally to this work

Introduction

Microglia colonize the central nervous system (CNS) during development, originating from uncommitted c-Kit$^+$ stem cells found in the yolk sac (Kierdorf et al., 2013). These c-Kit$^+$ cells develop into CD45$^+$/c-Kit$^-$/CX3CR1$^+$ cells that migrate to the CNS and become microglia. The development of these cells is dependent upon Pu.1 and Irf8 (Kierdorf et al., 2013), as well as the colony stimulating factor 1 receptor (CSF1R; (Erblich et al., 2011; Ginhoux et al., 2010)). Following migration of these progenitors to the CNS, the blood brain barrier (BBB) forms, effectively separating the microglia from the periphery. Infiltration of peripheral monocytes or macrophages into the CNS does not occur under normal conditions (Ginhoux et al., 2010; Mildner et al., 2007), and thus, microglia form an autonomous population.

The CSF1R is expressed by macrophages, microglia, and osteoclasts (Patel and Player, 2009) and has two natural ligands – CSF1 and IL-34 (Lin et al., 2008). CSF1 regulates the proliferation, differentiation, and survival of macrophages (Patel and Player, 2009), with mice lacking either CSF1 or the CSF1R showing reduced densities of macrophages in several tissues (Li et al., 2006). Furthermore, CSF1R knockout mice are devoid of microglia (Erblich et al., 2011; Ginhoux et al., 2010) and die before adulthood. In the brain, it has been demonstrated that microglia are the only cell type that expresses the CSF1R under normal conditions (Erblich et al., 2011; Nandi et al., 2012a). In this study, we investigate the effects of CSF1R inhibitors on microglial function, and find that inhibition leads to the elimination of virtually all microglia from the adult CNS, with no ill effects or deficits in behavior or cognition. Withdrawal of the inhibitor leads to the rapid repopulation with new cells that then differentiate into microglia. Notably, repopulation occurs rapidly from nestin expressing cells found throughout the CNS, representing a microglial progenitor cell.

Results

Selective CSF1R kinase inhibitors block growth of EOC 20 microglial cells *in vitro*

The EOC 20 microglial cell line has been shown to depend on the addition of spent media from LADMAC cells that produce CSF1. We tested several selective CSF1R kinase inhibitors (PLX3397 (Artis DR, July 28, 2005), PLX647 (Zhang et al., 2013), Ki20227 (Ohno et al., 2006) and GW2580 (Conway et al., 2005), and the non-selective kinase inhibitor dasatinib) on EOC 20 cells grown with either LADMAC spent media or conventional media, to which purified CSF1 was added (Supplemental Fig. 1A; conventional media + CSF1 shown). In both cases, the inhibitors completely arrested cell growth, as determined by a standard ATP assay (Crouch et al., 1993), with IC_{50} values below 1 μM (Supplemental Fig. 1B) and PLX3397 showing the most robust inhibition of all of the compounds tested.

CSF1R inhibitors dramatically reduce microglia numbers in the adult brain

For the initial *in vivo* experiments, all drugs were tested at very high doses, since their ability to penetrate the blood brain barrier was unknown. Based on our *in vitro* experiments, we selected PLX3397 for our *in vivo* work, as its IC_{50} values have been published and

shown to potently and selectively inhibit CSF1R and c-Kit over most other kinases (DeNardo et al., 2011). In addition, the effects of PLX3397 on peripheral myeloid cells have been extensively characterized (Abou-Khalil et al., 2013; Chitu et al., 2012; Coniglio et al., 2012; DeNardo et al., 2011; He et al., 2012; Mok et al., 2013; Prada et al., 2013), where chronic PLX3397 treatment eliminates tumor-associated macrophages, but has only modest effects on macrophage numbers in other tissues in wild-type mice (Mok et al., 2013). We also tested the PLX3397 analog, PLX647 (Zhang et al., 2013). PLX3397 or PLX647 were mixed into a standard rodent diet at 1160 and 1000 mg drug per kg chow, respectively, corresponding to doses of approximately 185 and 160 mg/kg body weight, and administered to an LPS (0.5 mg/kg) mouse model of neuroinflammation (Supplemental Fig. 1C). Brains were homogenized and Western blots were performed using anti-IBA1, a marker for microglia. As expected, LPS-treated mice were found to have elevated steady state levels of IBA1, consistent with increased neuroinflammation (Supplemental Fig. 1D, E). Treatment with either CSF1R antagonist prevented this LPS-induced IBA1 increase, suggesting that CSF1R signaling is essential for this neuroinflammatory effect. However, quite surprisingly, in the case of PLX3397 treatment, the IBA1 protein levels decreased to 70% below the levels of the PBS-treated controls. Immunostaining for IBA1 in the cortex of these animals confirmed these results and further revealed a clear decrease in microglia numbers with inhibitor treatments (Supplemental Fig. 1F, G), with remaining microglia exhibiting an enlarged morphology with thickened processes.

Based on these results, PLX3397 produced the most robust reductions in brain microglia. Next, we sought to administer decreasing concentrations of the compound in chow to determine a dose regimen for chronic studies. As before, 2 month-old male mice were treated with vehicle, LPS, or LPS + PLX3397 for 7 days (n = 4 per group). Western blot analysis of brain homogenates again showed a robust reduction in steady state levels of IBA1 at all doses, with 290mg/kg chow PLX3397 still showing maximal effects (Supplemental Fig. 1H, I).

Having determined the optimal dosing for all future chronic studies, we treated 12 month-old wild-type mice with 290mg/kg chow PLX3397 for 0, 1, 3, 7, 14, or 21 days (n = 4–5 per group). Immunostaining for IBA1 showed a robust, time-dependent reduction in microglia number, with a 50% reduction in microglia after just 3 days of treatment, and brains were essentially microglia-devoid by 21 days in all regions surveyed (Fig. 1A–F and 1J–N, with quantification in Fig. 1O). Morphological analyses of surviving microglia revealed a larger cell body (Supplemental Fig. 2E), an increased thickness of processes (Supplemental Fig. 2F) typically associated with a more phagocytotic phenotype (Neumann et al., 2009), and a reduction in the number of branches per microglia (Supplemental Fig. 2H). To determine if the results could simply be due to downregulation of the IBA1 microglial marker, we treated 2 month-old CX3CR1-GFP$^{+/-}$ mice with PLX3397. These mice express GFP in myeloid lineage cells (e.g., microglia and macrophages). After only 3 days treatment, GFP^{+} cells were counted in a 10X field of view from the hippocampus, cortex, and thalamus (n = 3 per group), showing >50% reduction in cell numbers (Fig. 1R–S).

Microglial death with CSF1R inhibition

Given the rapid depletion of microglia from the brain, we reasoned that blocking CSF1R signaling must result in microglial cell death, rather than just an inhibition of proliferation. Thus, we looked for evidence of microglial cell death. We further reasoned that dying and dead microglia would be most present at 3 and 7 days of PLX3397 treatment, as most microglia are eliminated within the first week. Indeed, we found many examples of $IBA1^+$ staining that looked like remnants of cells (Fig. 1P, Q, indicated by arrows). Given the enlarged size of surviving microglia during CSF1R inhibition, we hypothesize that these cells may be highly phagocytotic and involved in the clearing of microglial corpses from the CNS. However, few remnants were seen at 21 days of treatment, suggesting that the CNS has an additional microglia-independent method for eliminating cellular debris. To confirm that microglia undergo cell death with CSF1R inhibition, we found that many microglia stained for active caspase 3 in the same animals, a classic marker of apoptosing cells (Supplemental Fig. 2J–L). Further evidence of microglial death with CSF1R inhibition, as opposed to differentiation into alternative cell types, is shown in Figure 8 and accompanying text.

We then conducted a 7-day treatment in 2 month-old CX3CR1-$GFP^{+/-}$ mice and then performed flow cytometry on processed whole brains. GFP^+ cell counts revealed a 90% reduction with 7 days of PLX3397 treatment (Fig. 1T). In addition, more than 20% of these GFP^+ cells stained positively for propidium iodide (PI), indicative of dying microglia (Fig. 1U). We also performed stereological volume measurements of mice treated for 7 days with PLX3397 and found no significant differences, despite the loss of >90% of microglia (Fig. 1V).

To further show that microglia are dependent upon CSF1R signaling for their survival, we treated 2 month-old wild-type mice with PLX3397 or vehicle for 7 days (n = 4 per group) and counted the number of microglia, as well as mRNA levels for microglial markers (Fig. 2A–D). PLX3397 treatment reduced microglia numbers in the hippocampus, cortex, and the thalamus by >90%, as determined by automated counts of $IBA1^+$ cell bodies (Fig. 2A–C). mRNA levels of the microglial markers *AIF1* (which encodes IBA1), *CSF1R*, *CX3CR1*, *FCGR1*, *ITGAM*, and *TREM2* were all significantly reduced (Fig. 2D). Of the two CSF1R ligands, which are both produced by neurons, *CSF1* was unchanged while *IL*-34 was upregulated (Greter et al., 2012; Nandi et al., 2012b).

Effects of microglial depletion on other CNS cell types

We explored the effects of treatment on other CNS cell types by probing for steady state levels of astroctytic, oligodendrocytic, and neuronal markers via Western blot (Supplemental Fig. 3A, B). No changes in markers NeuN, MAP2, or Olig2 were observed. However, robust increases in the astrocytic markers GFAP and S100 were found. *GFAP* mRNA levels were also increased with 7 days of PLX3397 treatment, as measured via Real Time PCR (Supplemental Fig. 3C). To further investigate these changes in astrocytic markers, we performed immunofluorescent stains for GFAP at all treatment timepoints. GFAP cell counts showed no differences with treatment, despite the measured increases in mRNA and protein (Supplemental Fig. 3D–G). Likewise, S100 cell counts also revealed no

differences (Supplemental Fig. 3G). No changes in signal intensity with either GFAP or S100 were measured, and likewise, morphological analyses revealed no changes in astrocyte cell body volumes, process lengths, or diameters (Supplemental Fig. 3H–P). Thus, depletion of microglia results in increased mRNA and protein for astrocytic markers, but no changes in cell numbers or morphology.

Elimination of microglia does not affect the blood brain barrier

We tested if microglial-elimination could compromise the integrity of the BBB, using Evans Blue. No Evan's blue was found in the brain and there were no changes in peripheral organs in either control (n = 4) or microglia-depleted (n = 4) mice (Supplemental Fig. 2M and N), showing that the BBB remains intact.

Short- or long-term microglia depletion does not affect cognition or behavior

2 month-old wild-type mice were treated for 21 days with PLX3397 or vehicle (n = 10 per group). This treatment regimen was found to deplete >99% of all microglia from the brain, as illustrated in Supplemental Fig. 4A and B. Mice were first tested on the elevated plus maze (Supplemental Fig. 4C, D). Microglia-depleted mice spent significantly more time in the closed arms of the maze, which is typically considered an ethologically relevant behavior in rodents, and could be indicative of increased anxiety. No differences in the number of arm entries into either the closed or open arms were observed. Despite these changes in the elevated plus maze, open field analysis revealed no change in the amount of time spent in the center of the field, showing that microglia-depleted mice did not have increased anxiety in this task (Supplemental Fig. 4G). Additionally, no changes in the distance traveled or velocity were seen (Supplemental Fig. 4E, F), indicating that there were no locomotor differences between groups. Microglial elimination throughout the CNS had no effects on learning and memory, as determined via acquisition and probe trial of the Barnes maze (Supplemental Fig. 4H, I) or on locomotion, as tested with the accelerating rotarod (Supplemental Fig. 4J). Given these results in mice depleted of microglia for 21 days, we then set out to determine if further long-term depletion of microglia would alter cognition or behavior, as perhaps deficits would take longer than 3 weeks to manifest. To that end, wild-type mice were treated with PLX3397 or vehicle for 2 months, and then cognition and behavior assessed. A third group was administered the cholinergic antagonist scopolamine on testing days to induce cognitive deficits as a positive control (n = 10 per group). With long-term microglial elimination, no changes in elevated plus maze were observed (Fig. 2E, F). Likewise, no changes were seen in open field (Fig. 2G–I) or accelerating rotarod (Fig. 2L). Intriguingly, training on the Barnes maze revealed that microglia-depleted mice were able to learn the task significantly better than microglia-intact animals, as shown by shorter escape latencies on days 2 and 3 of training (Fig. 2J), as well as an overall reduction in average escape latency across all training days (Fig. 2K). Mice treated with scopolamine were unable to learn the task, as evidenced by an inability to escape the maze more quickly on subsequent days (Fig. 2J). No differences were found in the probe trial (data not shown). We then performed contextual fear conditioning, an additional hippocampal-dependent learning and memory task. No significant differences were found between microglia-depleted mice and microglia-intact mice, while mice treated with scopolamine performed significantly worse, and therefore showed a cognitive deficit as

expected (Fig. 2M). Thus, mice depleted of microglia for either 21 days or 2 months show no deficits in learning, memory, motor function, or behavior, and surprisingly, mice chronically depleted of microglia showed some evidence of enhanced learning.

Immune profiling of the microglia-depleted brain

To explore how the microglia-depleted brain responds to immune challenges, we treated 2 month-old wild-type mice for 7 days with PLX3397 to deplete their microglia (Fig. 3A–F). We then administered either PBS or LPS (0.25mg/kg) and sacrificed the animals 6 hours later. mRNA was extracted from whole brains, converted to cDNA, and then analyzed against a panel of 86 immune-related genes (Fig. 3G–I). Overall, depletion of microglia leads to robust reductions in the expression of many inflammatory genes, including *TNF-α* and other cytokines. Microglia-expressed genes are also robustly reduced, including *CD4, CD68, CD86, H2-Eb1* (which encodes MHC II), and *PTPRC* (which encodes CD45), reinforcing the finding that microglia are absent from these treated brains. Responses to LPS are dampened for many genes, but chemokine responses are mixed. Additionally, these results demonstrate that microglial elimination is not accompanied by an inflammatory response by the remaining cells in the CNS, which is an important feature of the approach to microglial-depletion shown here.

Rapid restoration of CNS microglia following drug removal

18 month-old wild-type mice were treated with PLX3397 for 28 days to eliminate microglia, to first show that microglia are still dependent upon CSF1R signaling in the aged brain, and secondly, to explore microglial homeostasis in the aged brain. At this point, all mice were switched to vehicle chow, and sacrificed 0, 3, 7, 14, and 21 days later to assess any microglial repopulation (n = 4 per group; Fig. 4A). Remarkably, within 3 days $IBA1^+$ cells appear throughout the brain with very different morphologies to resident microglia in control brains (Fig. 4B, D). They are much larger, with only short stubby processes. By 7 days recovery, the total number of microglia exceeds that of control mice, and their morphologies lie between that of the cells seen at 3 days and untreated microglia (Fig. 4B–H). By 14 days recovery, the microglia numbers stabilize to untreated levels and the repopulating microglia resemble normal ramified microglia. Thus, repopulation of the microglia-depleted brain occurs through rapid increases in cell numbers and differentiation into microglial morphologies. The cells seen at the 3-day recovery timepoint are unique – they are much larger than resident ramified microglia (Fig. 4I) and appear throughout the CNS, rather than in discrete locations (Supplemental Fig. 5). Curiously, we also found that these cells express a number of markers not seen in microglia in control brains, nor in surviving microglia while being treated (Fig. 4K). They are very strongly positive for the lectin IB4, as well as CD45. Many of these cells are $Ki67^+$ (a marker of cell proliferation) and $CD34^+$ (a marker of HSCs), while around 10% of these cells also show c-kit staining, another HSC marker. The majority of cells are also $nestin^+$ (a neuroectodermal development marker), a surprising finding given the myeloid lineage of microglia. However, at day 7, $IBA1^+$ cells assume a more typical microglia morphology, have repopulated the entire CNS, and are CD45, IB4, CD34, c-kit, nestin, and Ki67 negative. By 14 days, cells are morphologically indistinguishable from resident microglia in control brains and have comparable numbers (Fig. 4H). Thus, the adult CNS has a highly plastic and dynamic

microglial population that can be entirely repopulated following microglial elimination, even in the aged brain. mRNA profiling of these brains shows loss of microglia markers with CSF1R inhibition, consistent with microglia elimination, followed by recovery consistent with repopulation (Supplemental Fig. 6A). Additionally, large increases in the chemokines *CCL2, CCL3,* and *CCL5* were also seen at the 3-day recovery timepoint, suggesting strong signaling for repopulation to occur. Counts of repopulating microglia at the 3-day recovery timepoint showed that 3 mice had robust repopulation, while 2 mice still lacked microglia (Fig. 4H). mRNA levels of *AIF1* reflected these microglia counts, prompting us to perform correlations between *AIF1* levels and *CCL2, CCL3,* and *CCL5* (Supplemental Fig. 6B–G). Strong and highly significant correlations were found between *AIF1* levels and *CCL2* and *CCL5* during the early stages of repopulation (day 3), which trended toward significance for *CCL2* at day 7. As microglial depletion does not alter either *CCL2* or *CCL5* (Supplemental Fig. 6A), these increases in chemokines are a consequence of the repopulation process rather than just the reappearance of microglia.

Early microglial repopulation events highlight robust nestin-expressing cells

We next set out to explore the early repopulation events that occurred between drug withdrawal and the 3-day recovery timepoint. We treated 2 month-old CX3CR1-GFP$^{+/-}$ mice with PLX3397 for 7 days and then withdrew the drug for 0, 1, 2, or 3 days (n = 4 per group; Fig. 5A). Seven days of PLX3397 treatment eliminated ~70% of microglia in these CX3CR1-GFP$^{+/-}$ mice (Fig. 5B–F). Microglia continued to be eliminated until day 2 of recovery, but by day 3, the microglia population was quadrupled from that of the previous day (Fig. 5H). These data highlight a critical period of 48–72 hours for microglial repopulation, which is consistent with the results from the 18 month-old mice (Fig. 4). Measurements of PLX3397 in brain tissue revealed that the drug was quickly cleared from the brain, with trace amounts being detected by 1-day recovery (Fig. 5I). Thus, microglial elimination continues in the absence of drug. We also performed flow cytometry for GFP$^+$ cells from the liver and spleen to look at the effects in the periphery (Fig. 5G). No significant changes in GFP$^+$ cell numbers were seen in the liver with either treatment or repopulation, while some reductions were seen in the spleen by day 2 of recovery, but increased again the following day. In accordance with Figure 4, we found that the microglia were strongly positive for IB4 at the 2- and 3-day recovery timepoints (Supplemental Fig. 7A), but curiously, repopulating cells were negative for CD34 and c-Kit in these younger animals (data not shown). Additionally, we explored the microglial transcription factor Pu.1, which is important for myeloid lineage cells to differentiate from progenitors (Kueh et al., 2013), and found that staining is markedly increased in microglia at the 2- and 3-day recovery timepoints (Supplemental Fig. 7B). As in the 18 month-old mice, repopulating microglia are strongly nestin$^+$ at the 2- and 3-day recovery timepoints (Fig. 5J), with no expression seen in the other groups. Indeed, Western blot of whole brain homogenates revealed a dramatic increase (1,000%) in steady state levels of nestin at day 3 of recovery (Fig. 5K and quantified in L). We also probed for steady state levels of CSF1R, which are reduced at recovery days 0, 1, and 2, but are restored by recovery day 3. Additionally, the monocyte marker CCR2 revealed no changes, suggesting that repopulation does not occur from peripheral monocytes.

Microarray analysis of microglia-depleted and repopulating brains reveals cell proliferation

To gain insight into the origin(s) and properties of repopulating cells, we conducted microarray analysis of mRNA extracted from whole brains of control, recovery day 1, and recovery day 3 groups. We selected recovery day 1 as a time point at which microglia are eliminated and the drug is cleared from the system (Fig. 5H, I). Significant changes in gene expression were determined by Cyber T analysis and ranked in order of significance, with the top 30 gene expression changes shown in Supplemental Fig 8A–C. Reductions in known microglial-associated genes were most common in the 1-day recovery group compared to controls, including recently identified microglial selective genes *p2ry13, Siglech,* and *slc2a5* (Chiu et al., 2013; Gautier et al., 2012). Additionally, reductions in *CSF1R, ITGAM,* and *CX3CR1* were observed, consistent with Real Time PCR data shown in Fig. 2D. To build a gene expression profile of the repopulating brain and cells, we compared both day-1 recovery (microglia remain depleted) and control brains to day-3 recovery (repopulation has just begun to occur). In both comparisons, changes in gene expression associated with cell proliferation and cell cycle control were highly prevalent (Supplemental Fig. 8B, C), including *mki67,* as well as *Ube2c, Ccna2, Prr11,* and *Top2a.* Thus, the expression profile of the repopulating brain supports the notion that repopulation occurs as a result of proliferation. Additionally, we compared expression of significantly changed myeloid genes in recovery day 1 (microglia-depleted) against recovery day 3 (repopulating) in order to determine the expression pattern of the repopulating cells (Supplemental Fig. 8D). Myeloid genes were increased, as expected. However, several microglial-specific genes have been recently identified that are not expressed in macrophages, and we found that these markers were also significantly increased, including *F11r, Gpr165, Gpr84, Olfml3, Serpine2,* and *Siglech* (Chiu et al., 2013; Gautier et al., 2012). The microglial-specific gene *Tmem119* was not detected via microarray. However, Real Time PCR of mRNA extracted from 3-day repopulating brains revealed increases for both microglial-specific genes *Tmem119* and *Siglech* (Supplemental Fig. 9C), as well as *Aif1, CSF1R, Cx3cr1,* and *Trem2,* providing validation of the microarray data. We also looked at macrophage-specific genes in the microarray dataset including *Fn1, Slp1, Saa3, Prg4, Cfp, Cd5L, GM11428, Crip1Pf4,* and *Alox15* (Gautier et al., 2012), but found no significant changes (data not shown). Additionally, the monocyte-specific marker *CCR2* was not changed. Thus, these data support the notion that repopulating cells have an expression profile of microglia and not of peripheral myeloid cells, and that they are derived from proliferation rather than infiltration.

Fate mapping with BrdU reveals that repopulating microglia derive from non-microglial nestin^{+} progenitor cells

Having determined that repopulation occurs from cell proliferation rather than infiltration, we next stained tissue using Ki67 as a marker of cell proliferation in our early repopulation time course in CX3CR1-GFP$^{+/-}$ mice. At the 2-day recovery timepoint, the brain contains many microglia-negative (GFP^{-}/Ki67^{+}) cells throughout, often with 2 adjacent nuclei, which are not seen in control, 0-, or 1-day recovery brains (Fig. 6A, B with quantification in C–E). By 3 days of recovery, most Ki67^{+} cells are now also GFP^{+}, suggesting that these Ki67^{+} cells are potential microglia progenitors.

Proliferating cells can be labeled with the thymidine analog BrdU, thus allowing us to mark the Ki67$^+$/proliferating cells and track their fate, to determine if they do indeed become microglia. To that end, we tagged proliferating cells with BrdU (single injection IP) at the 2-day recovery timepoint (Fig. 7A–H). Mice were sacrificed 5 hours later and their brains were analyzed to confirm that the non-microglial proliferating cells incorporated BrdU. Indeed, 5 hours post-injection, many non-microglial cells had incorporated BrdU (Fig. 7B, C; IBA1$^-$), while only 30% of all BrdU$^+$ cells expressed microglial markers (Fig 7B, C with quantification in G, H). BrdU is not incorporated into appreciable numbers of cells in control animals (Fig. 7A and quantified in G, H) or in those depleted of microglia and still on inhibitor (data not shown). Thus, these BrdU-incorporated non-microglial cells correspond to the potential microglia progenitor cells. Having determined that the potential progenitor cells incorporate BrdU, we then repeated the experiment, but sacrificed animals 24 hours after BrdU administration, rather than 5 hours, in order to track their fate. After 24 hours, virtually all BrdU-incorporated cells were microglia (as determined by IBA1; Fig. 7E, F and quantified in G, H), with very few BrdU$^+$/IBA1$^-$ cells observed (Fig. 7H). These results demonstrate that the non-microglial proliferating/BrdU-incorporating cells become microglia within 24 hours, and confirm these cells as microglial progenitors.

Given these findings of potential microglial progenitor cells stimulated to proliferate and then differentiate into microglia, we reasoned that these progenitors must express some of the markers that the initial repopulating microglia express, such as nestin. Indeed, co-staining for Ki67 and nestin in 2-day repopulating brains revealed that these newly appeared proliferating cells express nestin, with fine processes radiating out from a cell body (Fig. 7K–N, with magnified images in L and N), lending further credence to the idea that these proliferating nestin-expressing cells become the repopulated microglia. As controls, we show that these cells do not express either GFAP (Fig. 7I) or MAP2 (Fig. 7J). Finally, we confirmed that the BrdU-incorporated non-microglial cells found 5 hours after BrdU administration (Fig. 7B) also expressed nestin (Fig. 7O, P). These BrdU-incorporated cells lack the extensive nestin$^+$ processes seen in Figure 7K–N, suggesting the cells are between the stages of DNA synthesis and mitosis/cytokines is, unlike the Ki67$^+$/nestin$^+$cells that had completed cell division (Fig. 7K–N).

Surviving microglia cannot solely account for repopulation

While not all microglia are eliminated with CSF1R inhibition, the numbers and rates of repopulation cannot support repopulation solely from these few surviving cells. Our data from Figure 5 shows that repopulation begins after 48 hours following drug withdrawal and that there is a substantial increase in repopulating cells by 72 hours. In fact, the average number of microglia per section quadruples from approximately 950 cells at 48 hours to roughly 3,700 by 72 hours. Proliferation from the surviving 950 cells alone would be unlikely to produce 3,700 cells within 24 hours. In this experiment, only ~70% of microglia were eliminated; however, we see faster rates of repopulation with >95% elimination (as shown in Supplemental Fig. 9AC). Here, repopulation occurred at a tremendous rate, with ~14,000 cells/slice present at 72 hours, despite only ~600 cells/slice being present in the depleted brains. If the surviving microglia were to be the only source of repopulation each surviving cell would have to proliferate every 5–6 hours (Supplemental Fig. 9D), with no

reductions in cell size and with constant migration away from daughter cells, in order to account for complete repopulation. The presence of a progenitor cell in the brain could, however, account for the rapid repopulation observed.

Microglia repopulation does not occur from peripheral cells

Our data show the presence of a microglial progenitor cell in the adult CNS that can proliferate and then differentiate into the repopulating microglia. However, we also wished to rule out fully the possibility that peripheral cells were able to cross the BBB and also contribute to repopulation. To that end, we performed 2 experiments. Firstly, pharmacokinetic (PK) data revealed that only ~5% of plasma PLX3397 enters the CNS, rendering peripheral concentrations ~20X higher. We setout to establish if repopulation could still occur with concentrations of PLX3397 that block CSF1 receptors in the periphery, but not in the CNS, as repopulation is dependent upon withdrawal of the CSF1R inhibitor. We treated 2 month-old wild-type mice with 290mg/kg chow PLX3397 for 14 days to deplete microglia. At this point, this dose was replaced with chow containing 0, 16, 32, 75, 150, or 290 mg/kg PLX3397 (n = 3 per group; Supplemental Fig. 10A). Three days later, mice were sacrificed and half brains taken for PK and mRNA analyses, and repopulation assessed. Plasma and brain PLX3397 levels were measured for each of the groups (Supplemental Fig. 10B), showing that even in the 16 mg/kg group, the plasma PLX3397 concentration was greater than that found in the brain in the 290 mg/kg group (i.e., the concentration needed for microglial elimination). Brain PLX3397 concentrations were very low, with 0.5 – 0.1 μM measured in the 75 mg/kg and lower dose groups. Repopulation (as assessed by *CSF1R* and the microglia-specific markers *Siglech* and *Tmem119*) occurred in the 0, 16, 32, and 75 mg/kg groups, but not in the 150 or 290 mg/kg groups, despite peripheral PLX3397 concentrations being much higher than that found in the brains of the 290 mg/kg group (Supplemental Fig. 10B). From these findings, we conclude that repopulation cannot occur from peripheral cells, but must occur from within the CNS.

Secondly, while we have already determined that brain-wide CCR2 levels are not altered with repopulation (Fig. 5K, L), we further set out to determine if infiltration of monocytes could represent a source of repopulating cells. To that end, we treated CCR2-RFP$^{+/-}$ mice with PLX3397 for 7 days, and withdrew drug for 5 days to stimulate repopulation (n = 4 per group). Monocytes specifically express RFP in these mice (Saederup et al., 2010), which we confirmed in the blood of these animals (sample shown is obtained from a CCR2-RFP$^{+/-}$ x CX3CR1-GFP$^{+/-}$ mouse; Supplemental Fig. 10D). However, we were unable to find any RFP-expressing cells within the CNS of control, microglia-depleted, or repopulated animals (Supplemental Fig. 10E), despite robust microglial repopulation, confirming that the repopulating cells do not derive from monocytes. We were able to find a handful of RFP positive cells in the 12 brains examined, and these were always found within blood vessels, such as that shown in Supplemental Figure 10F. To further rule out the possibility of monocytes contributing to repopulation, we also performed immunostains for CCR2 in repopulating brains at 0, 1, 2, and 3 days recovery in the event that monocytes were able to enter the CNS and then rapidly differentiate into microglia (Supplemental Fig. 10G). While neurons stained positive for CCR2, which has been previously reported (Banisadr et al., 2005; van der Meer et al., 2000), none of the repopulating cells were CCR2 positive. We

also performed stains for T-cells (anti-CD3) and dendritic cells (anti-CD11c), but found no evidence for either cell type in the repopulating brains (data not shown).

Fate mapping reveals that microglia do not dedifferentiate into alternative cell types with CSF1R inhibition and that repopulated cells are fully dependent upon CSF1R signaling

An additional hypothetical explanation for repopulation is that microglia are not actually dying with CSF1R inhibition, but dedifferentiating into an alternative cell type, which then redifferentiates back into microglia upon removal of the inhibitor. To address this, we have first determined that repopulating cells are also fully dependent upon CSF1R signaling, as repopulating microglia strongly express the CSF1R (Fig. 8A). We treated 2 month-old wild-type mice with PLX3397 for 21 days to deplete microglia ("on", n = 4). An additional group was then allowed to repopulate for 14 days ("on-off", n = 5), and a final group was then treated again with PLX3397 for 7 days ("on-off-on", n = 5). As shown in Figure 8C and D, 21 days of PLX3397 treatment eliminated >99% of all microglia from the CNS, and 14 days recovery restored numbers of microglia back to resident microglial levels. Crucially, treatment of repopulated microglia with PLX3397 eliminated >95% of microglia, showing that these cells are also dependent upon CSF1R signaling for their survival.

Next, to track the fate of microglia during CSF1R inhibition, we tagged repopulating microglia with BrdU (as depicted in Figure 8E), via treatment with PLX3397 for 7 days, followed by 7 days recovery, during which BrdU was administered daily. As expected, repopulating microglia incorporated BrdU (Figure 8G and quantified in H). Once repopulating microglia were tagged with BrdU, we treated mice with PLX3397 for 7 days and then explored the CNS for BrdU-labeled cells. This second treatment eliminated >80% of microglia, including BrdU-incorporated cells (Fig. 8H and quantified in I), thus confirming that microglia are being eliminated from the CNS, rather than differentiating into a non-microglial cell type.

Discussion

Dependence of microglia on CSF1R signaling in the adult brain

Recent studies have highlighted the importance of the CSF1R to the development of microglia, with mice lacking the CSF1R being born devoid of microglia (Erblich et al., 2011; Ginhoux et al., 2010). Unfortunately, these mice have developmental defects and usually die by adulthood, by which time some microglia are observed (Erblich et al., 2011). Mice lacking either of the two CSF1R ligands, CSF1 (Wegiel et al., 1998) or IL-34 (Wang et al., 2012), also have reduced densities of microglia throughout the CNS. Thus, the CSF1R is heavily implicated in the development of microglia. However, it is unknown what role the CSF1R plays in microglia homeostasis and viability in the adult brain. Our results show that microglia in the adult brain are fully dependent upon CSF1R signaling for their survival and that we can eliminate virtually all microglia from the CNS for extended periods of time through the administration of CSF1R inhibitors. Thus, CSF1R signaling appears to act as a requisite growth factor receptor for microglia and its blockade drives microglia to their death. Growth factor withdrawal is known to induce apoptosis in many other cell types, including HSCs (Cornelis et al., 2005) and macrophages (Chin et al., 1999). Consequently,

we can take advantage of this dependency to manipulate microglial levels in the adult brain through administration of CSF1R inhibitors, allowing studies into microglia function that have not been possible before. Moreover, the CSF1R provides an ultimate drug target for neuroinflammation, in that we can now eliminate microglia rather than just suppress aspects of their activity.

Role of microglia in the healthy adult brain

We set out to determine if microglia play an important role in cognition and behavior in healthy adult mice. Chronic depletion of >99% of all microglia for 3 or 8 weeks in adult mice resulted in no deficits in any behavioral cognitive task administered, including Barnes maze (a test of spatial learning and memory). In fact, mice depleted of microglia for 8 weeks learned to escape the Barnes maze significantly faster than control animals. Finally, no motor deficits were observed in treated mice as determined by accelerating rotarod testing and open field. Therefore, these results show that microglia are not overtly important in these cognitive tasks – a surprising finding given the numerous physical interactions between neurons and microglia, as well as the secreted factors that are released from microglia. While our results show that microglia are not overtly necessary for these behaviors, previous studies have shown that microglia are crucial during development, with CX3CR1-GFP mice showing a transient reduction in microglia during development (Zhan et al., 2014), leading to long-term deficits in behavior (Zhan et al., 2014), memory, and LTP (Rogers et al., 2011). Of note, a recent study found that short-term depletion of microglia, via genetic expression of diphtheria toxin receptor and subsequent diphtheria toxin administration for ~7 days, led to deficits in learning, including contextual fear conditioning (Parkhurst et al., 2013). We do not find these deficits in our mice, despite lacking microglia for 2 months. These differences may be accounted for by the method of microglia-elimination and the acute response of the CNS and surviving microglia to massive microglial-death via diphtheria toxin, while the response of the immune system in our paradigm may be more suppressed due to CSF1R inhibition. This study also reported slower repopulation than we see, which may be accounted for by the different methods of microglial-elimination and the time-scales involved that likely activate different signaling pathways within the brain. As administration of CSF1R inhibitors is potentially translatable to humans for modulation of microglia numbers, a lack of negative effects on cognition is an important observation.

Rapid repopulation of the microglia-depleted brain

Having shown that we could eliminate >99% of all microglia from the adult brain, we asked the question of whether new cells could replace the lost microglia and repopulate the CNS. Microglia colonize the CNS during development, before E9 (Ginhoux et al., 2010). Once the CNS has formed, these microglia are long-lived and have the capacity to divide and self-renew in an autonomous cell population, but the dynamics and regulation of resident microglia numbers are not fully understood. In the periphery, macrophage populations are thought to be replenished by circulating monocytes derived from multipotent hematopoietic stem cells found in the bone marrow, although this view has been recently challenged (Hashimoto et al., 2013; Sieweke and Allen, 2013). In contrast, the brain is separated from circulation by the BBB, and experiments have shown that there is little infiltration of

peripheral HSCs/monocytes/macrophages into the CNS to help maintain or replenish microglia under normal, non irradiated conditions (Ajami et al., 2011; Greter and Merad, 2013; Mildner et al., 2007). Thus, we set out to explore if repopulation could occur in the adult brain, as well as the consequences of withdrawing CSF1R antagonists once microglia were depleted.

We initially predicted that the brain would remain absent of microglia for some time, given our current knowledge about the origins and proliferative properties of microglia, but remarkably, we found that the CNS can fully repopulate with new microglia within just 7 days. Furthermore, the returning number of microglia is identical to that in untreated mice, showing astonishing and precise regulation of the microglial population within a very short period of time. Repopulating microglia derive from proliferation, as shown with Ki67 expression and incorporation of BrdU, rather than infiltration of peripheral cells into the CNS. Initially, repopulating microglia show very different morphologies and expression patterns to resident microglia, such as immunoreactivity for nestin, but rapidly differentiate into ramified microglia over a 7–14 day period. Crucially, we find that the repopulating brain induces the proliferation of nestin-expressing cells throughout the CNS, which appear to become the repopulating microglia. This finding helps to explain why these initial microglia strongly express nestin and how microglia numbers can be restored in a very short period of time, given that there are so few surviving microglia. It should be noted that the microglia themselves also proliferate, as evidenced by the expression of Ki67 and observations of cytokines is (i.e., Fig. 7A, 3-day recovery), revealing that repopulation may occur partly from nestin-expressing proliferating progenitors and partly from the cells that were nestin progenitors and have just become microglia, or from proliferation of surviving cells.

Of note, microglia are of a myeloid lineage rather than the neuroectodermal lineage that nestin expression would suggest, leading us to question why the repopulating microglia express nestin. In explaining this, it is possible to generate microglia from embryonic stem (ES) cells (Beutner et al., 2010) - ES cells are differentiated to a neuronal, nestin^{+} lineage and then the neuronal growth factors are removed, resulting in microglia. Hence, ES cells need to pass through a nestin^{+} stage on their way to becoming microglia, in line with the cells that we describe in this study, providing clear evidence that repopulating microglia strongly express nestin. Additionally, several previous studies have shown subsets of microglia to be able to express nestin under certain conditions, such as in culture (Yokoyama et al., 2004), following TBI (Sahin Kaya et al., 1999), or following optic nerve injury (Wohl et al., 2011) where proliferating, BrdU-incorporating microglia initially also express nestin. A recent study has also highlighted that the CSF1R negatively regulates the expansion of nestin^{+} progenitors in the developing brain, an intriguing parallel with our own findings in the adult brain and the relationship between CSF1R signaling and nestin expressing progenitors and microglia (Nandi et al., 2012b). Thus, we show that the adult brain has a remarkable capacity to regulate and renew its microglia population, through previously undescribed microglial progenitor cells, and that the CSF1R plays a crucial role in microglial tissue homeostasis.

Materials and Methods

Refer to expanded methods in the supplement for additional details.

Compounds

PLX3397 and PLX647 were provided by Plexxikon Inc. and formulated in AIN-76A standard chow by Research Diets Inc. at the doses indicated in the text. PLX3397 was provided at 290 mg/kg, unless otherwise specified.

EOC 20 growth assays

EOC 20 microglial cells were grown either with the addition of LADMAC cell conditioned media, as a source of CSF1 as described (ATCC CRL-2469), or in DMEM containing recombinant CSF1. Cell numbers were quantified using ATPlite luminescence assay.

Animal Treatments

All rodent experiments were performed in accordance with animal protocols approved by the Institutional Animal Care and Use Committee at the University of California, Irvine (UCI). *LPS treatment:* LPS was administered intraperitoneally (IP). *Evans Blue dye administration:* to assess blood brain barrier integrity, mice were injected with Evans Blue dye (IP) and sacrificed 6 hours later. *BrdU labeling:* BrdU was administered via IP and mice sacrificed 5 or 24 hours later.

Immunoblotting

Brain homogenates and immunoblotting were prepared as previously described (Green et al., 2011). Quantitative densitometric analyses were performed on digitized images of immunoblots with Image J (NIH).

Immunostaining

Light-level immunohistochemistry was performed using an avidin-biotin immunoperoxidase technique and was visualized with diaminobenzidine, as previously described (Oddo et al., 2003).

Confocal microscopy

Fluorescent immunolabeling followed a standard indirect technique (primary antibody followed by fluorescent secondary antibody) as described in (Neely et al., 2011).

Flow Cytometry

Using a FACS Aria II, the viable cell population of interest from an unstained control was gated according to size and granularity based on forward and side scatter properties. Using these parameters, the percentage of GFP^+ cells, as well as GFP^+/PI^+ cells, were quantified for the CX3CR1-$GFP^{+/-}$ mice using FACS Diva Software.

Brain Volume

Brain volumes were obtained via Cavalieri measurements of every 6^{th} section per animal.

mRNA Extraction and Real Time PCR (RT-PCR)

Total mRNA was extracted from frozen half brains, cDNA was synthesized, and RT-PCR was performed with commercially available kits.

Behavioral testing

Mouse cognition and behavior were evaluated using the elevated plus maze, open field, Barnes maze, accelerating rotarod, and contextual fear conditioning.

Microarray

RNA was extracted and purified (as described above), then processed at the University of California, Irvine DNA and Protein MicroArray Facility using commercially available microarray cards.

Statistics

Appropriate statistical analyses were carried out to determine significance between groups (see supplemental information for specific tests employed).

Supplementary Material

Refer to Web version on PubMed Central for supplementary material.

Acknowledgments

Research reported in this publication was supported by the National Institute of Neurological Disorders and Stroke of the National Institutes of Health under Award Number 1R01NS083801 to KNG and F31NS086409 to RAR. Support was further provided through NIH award UL1TR000153, as well as the White hall foundation to KNG, the American Federation of Aging Research to KNG, and the Alzheimer's Association to KNG. ME is supported by NIH training fellowship AG00538. The content is solely the responsibility of the authors and does not necessarily represent the official views of the National Institutes of Health. BM, HN, and BLW are employees of Plexxikon Inc. We give thanks to Vanessa Scarfone, the Sue and Bill Gross Stem Cell Research Center Core Facility, and the CIRM Shared Research Lab for assistance with flow cytometry.

References

Abou-Khalil R, Yang F, Mortreux M, Lieu S, Yu YY, Wurmser M, Pereira C, Relaix F, Miclau T, Marcucio RS, et al. Delayed bone regeneration is linked to chronic inflammation in murine muscular dystrophy. J Bone Miner Res. 2013

Ajami B, Bennett JL, Krieger C, McNagny KM, Rossi FM. Infiltrating monocytes trigger EAE progression, but do not contribute to the resident microglia pool. Nat Neurosci. 2011; 14:1142–1149. [PubMed: 21804537]

Artis, DR.; BR; Gillette, S.; Hurt, CR.; Ibrahim, PL.; Zuckerman, RL. U.S. patent. Molecular scaffolds for kinase ligand development. USA: Jul 28. 2005

Banisadr G, Gosselin RD, Mechighel P, Rostene W, Kitabgi P, Melik Parsadaniantz S. Constitutive neuronal expression of CCR2 chemokine receptor and its colocalization with neurotransmitters in normal rat brain: functional effect of MCP-1/CCL2 on calcium mobilization in primary cultured neurons. J Comp Neurol. 2005; 492:178–192. [PubMed: 16196033]

Beutner C, Roy K, Linnartz B, Napoli I, Neumann H. Generation of microglial cells from mouse embryonic stem cells. Nat Protoc. 2010; 5:1481–1494. [PubMed: 20725065]

Chin BY, Petrache I, Choi AM, Choi ME. Transforming growth factor beta1 rescues serum deprivation-induced apoptosis via the mitogen-activated protein kinase (MAPK) pathway in macrophages. J Biol Chem. 1999; 274:11362–11368. [PubMed: 10196228]

Chitu V, Nacu V, Charles JF, Henne WM, McMahon HT, Nandi S, Ketchum H, Harris R, Nakamura MC, Stanley ER. PSTPIP2 deficiency in mice causes osteopenia and increased differentiation of multipotent myeloid precursors into osteoclasts. Blood. 2012; 120:3126–3135. [PubMed: 22923495]

Chiu IM, Morimoto ET, Goodarzi H, Liao JT, O'Keeffe S, Phatnani HP, Muratet M, Carroll MC, Levy S, Tavazoie S, et al. A neurodegeneration-specific gene-expression signature of acutely isolated microglia from an amyotrophic lateral sclerosis mouse model. Cell Rep. 2013; 4:385–401. [PubMed: 23850290]

Coniglio SJ, Eugenin E, Dobrenis K, Stanley ER, West BL, Symons MH, Segall JE. Microglial stimulation of glioblastoma invasion involves epidermal growth factor receptor (EGFR) and colony stimulating factor 1 receptor (CSF-1R) signaling. Mol Med. 2012; 18:519–527. [PubMed: 22294205]

Conway JG, McDonald B, Parham J, Keith B, Rusnak DW, Shaw E, Jansen M, Lin P, Payne A, Crosby RM, et al. Inhibition of colony-stimulating-factor-1 signaling in vivo with the orally bioavailable cFMS kinase inhibitor GW2580. Proc Natl Acad Sci U S A. 2005; 102:16078–16083. [PubMed: 16249345]

Cornelis S, Bruynooghe Y, Van Loo G, Saelens X, Vandenabeele P, Beyaert R. Apoptosis of hematopoietic cells induced by growth factor withdrawal is associated with caspase-9 mediated cleavage of Raf-1. Oncogene. 2005; 24:1552–1562. [PubMed: 15674327]

Crouch SP, Kozlowski R, Slater KJ, Fletcher J. The use of ATP bioluminescence as a measure of cell proliferation and cytotoxicity. J Immunol Methods. 1993; 160:81–88. [PubMed: 7680699]

DeNardo DG, Brennan DJ, Rexhepaj E, Ruffell B, Shiao SL, Madden SF, Gallagher WM, Wadhwani N, Keil SD, Junaid SA, et al. Leukocyte complexity predicts breast cancer survival and functionally regulates response to chemotherapy. Cancer Discov. 2011; 1:54–67. [PubMed: 22039576]

Erblich B, Zhu L, Etgen AM, Dobrenis K, Pollard JW. Absence of colony stimulation factor-1 receptor results in loss of microglia, disrupted brain development and olfactory deficits. PLoS One. 2011; 6:e26317. [PubMed: 22046273]

Gautier EL, Shay T, Miller J, Greter M, Jakubzick C, Ivanov S, Helft J, Chow A, Elpek KG, Gordonov S, et al. Gene-expression profiles and transcriptional regulatory pathways that underlie the identity and diversity of mouse tissue macrophages. Nat Immunol. 2012; 13:1118–1128. [PubMed: 23023392]

Ginhoux F, Greter M, Leboeuf M, Nandi S, See P, Gokhan S, Mehler MF, Conway SJ, Ng LG, Stanley ER, et al. Fate mapping analysis reveals that adult microglia derive from primitive macrophages. Science. 2010; 330:841–845. [PubMed: 20966214]

Green KN, Khashwji H, Estrada T, Laferla FM. ST101 induces a novel 17 kDa APP cleavage that precludes A beta generation in vivo. Ann Neurol. 2011; 69:831–844. [PubMed: 21416488]

Greter M, Lelios I, Pelczar P, Hoeffel G, Price J, Leboeuf M, Kundig TM, Frei K, Ginhoux F, Merad M, et al. Stroma-derived interleukin-34 controls the development and maintenance of langerhans cells and the maintenance of microglia. Immunity. 2012; 37:1050–1060. [PubMed: 23177320]

Greter M, Merad M. Regulation of microglia development and homeostasis. Glia. 2013; 61:121–127. [PubMed: 22927325]

Hashimoto D, Chow A, Noizat C, Teo P, Beasley MB, Leboeuf M, Becker CD, See P, Price J, Lucas D, et al. Tissue-resident macrophages self-maintain locally throughout adult life with minimal contribution from circulating monocytes. Immunity. 2013; 38:792–804. [PubMed: 23601688]

He Y, Rhodes SD, Chen S, Wu X, Yuan J, Yang X, Jiang L, Li X, Takahashi N, Xu M, et al. c-Fms signaling mediates neurofibromatosis Type-1 osteoclast gain-in-functions. PLoS One. 2012; 7:e46900. [PubMed: 23144792]

Kierdorf K, Erny D, Goldmann T, Sander V, Schulz C, Perdiguero EG, Wieghofer P, Heinrich A, Riemke P, Holscher C, et al. Microglia emerge from erythromyeloid precursors via Pu.1- and Irf8-dependent pathways. Nat Neurosci. 2013; 16:273–280. [PubMed: 23334579]

Kueh HY, Champhekhar A, Nutt SL, Elowitz MB, Rothenberg EV. Positive Feedback Between PU.1 and the Cell Cycle Controls Myeloid Differentiation. Science. 2013

Li J, Chen K, Zhu L, Pollard JW. Conditional deletion of the colony stimulating factor-1 receptor (c-fms proto-oncogene) in mice. Genesis. 2006; 44:328–335. [PubMed: 16823860]

Lin H, Lee E, Hestir K, Leo C, Huang M, Bosch E, Halenbeck R, Wu G, Zhou A, Behrens D, et al. Discovery of a cytokine and its receptor by functional screening of the extracellular proteome. Science. 2008; 320:807–811. [PubMed: 18467591]

Mildner A, Schmidt H, Nitsche M, Merkler D, Hanisch UK, Mack M, Heikenwalder M, Bruck W, Priller J, Prinz M. Microglia in the adult brain arise from Ly-6 ChiCCR2+ monocytes only under defined host conditions. Nat Neurosci. 2007; 10:1544–1553. [PubMed: 18026096]

Mok S, Koya RC, Tsui C, Xu J, Robert L, Wu L, Graeber T, West BL, Bollag G, Ribas A. Inhibition of CSF1 Receptor Improves the Anti-tumor Efficacy of Adoptive Cell Transfer Immunotherapy. Cancer Res. 2013

Nandi S, Gokhan S, Dai XM, Wei S, Enikolopov G, Lin H, Mehler MF, Richard Stanley E. The CSF-1 receptor ligands IL-34 and CSF-1 exhibit distinct developmental brain expression patterns and regulate neural progenitor cell maintenance and maturation. Dev Biol. 2012a

Nandi S, Gokhan S, Dai XM, Wei S, Enikolopov G, Lin H, Mehler MF, Stanley ER. The CSF-1 receptor ligands IL-34 and CSF-1 exhibit distinct developmental brain expression patterns and regulate neural progenitor cell maintenance and maturation. Dev Biol. 2012b; 367:100–113. [PubMed: 22542597]

Neely KM, Green KN, LaFerla FM. Presenilin is necessary for efficient proteolysis through the autophagy-lysosome system in a gamma-secretase-independent manner. J Neurosci. 2011; 31:2781–2791. [PubMed: 21414900]

Neumann H, Kotter MR, Franklin RJ. Debris clearance by microglia: an essential link between degeneration and regeneration. Brain. 2009; 132:288–295. [PubMed: 18567623]

Oddo S, Caccamo A, Shepherd JD, Murphy MP, Golde TE, Kayed R, Metherate R, Mattson MP, Akbari Y, LaFerla FM. Triple-transgenic model of Alzheimer's disease with plaques and tangles: intracellular A beta and synaptic dysfunction. Neuron. 2003; 39:409–421. [PubMed: 12895417]

Ohno H, Kubo K, Murooka H, Kobayashi Y, Nishitoba T, Shibuya M, Yoneda T, Isoe T. A c-fms tyrosine kinase inhibitor, Ki20227, suppresses osteoclast differentiation and osteolytic bone destruction in a bone metastasis model. Mol Cancer Ther. 2006; 5:2634–2643. [PubMed: 17121910]

Parkhurst CN, Yang G, Ninan I, Savas JN, Yates JR 3rd, Lafaille JJ, Hempstead BL, Littman DR, Gan WB. Microglia Promote Learning-Dependent Synapse Formation through Brain-Derived Neurotrophic Factor. Cell. 2013; 155:1596–1609. [PubMed: 24360280]

Patel S, Player MR. Colony-stimulating factor-1 receptor inhibitors for the treatment of cancer and inflammatory disease. Curr Top Med Chem. 2009; 9:599–610. [PubMed: 19689368]

Prada CE, Jousma E, Rizvi TA, Wu J, Dunn RS, Mayes DA, Cancelas JA, Dombi E, Kim MO, West BL, et al. Neurofibroma-associated macrophages play roles in tumor growth and response to pharmacological inhibition. Acta Neuropathol. 2013; 125:159–168. [PubMed: 23099891]

Rogers JT, Morganti JM, Bachstetter AD, Hudson CE, Peters MM, Grimmig BA, Weeber EJ, Bickford PC, Gemma C. CX3CR1 deficiency leads to impairment of hippocampal cognitive function and synaptic plasticity. J Neurosci. 2011; 31:16241–16250. [PubMed: 22072675]

Saederup N, Cardona AE, Croft K, Mizutani M, Cotleur AC, Tsou CL, Ransohoff RM, Charo IF. Selective chemokine receptor usage by central nervous system myeloid cells in CCR2-red fluorescent protein knock-in mice. PLoS One. 2010; 5:e13693. [PubMed: 21060874]

Sahin Kaya S, Mahmood A, Li Y, Yavuz E, Chopp M. Expression of nestin after traumatic brain injury in rat brain. Brain Res. 1999; 840:153–157. [PubMed: 10517963]

Sieweke MH, Allen JE. Beyond stem cells: self-renewal of differentiated macrophages. Science. 2013; 342:1242974. [PubMed: 24264994]

van der Meer P, Ulrich AM, Gonzalez-Scarano F, Lavi E. Immunohistochemical analysis of CCR2, CCR3, CCR5, and CXCR4 in the human brain: potential mechanisms for HIV dementia. Exp Mol Pathol. 2000; 69:192–201. [PubMed: 11115360]

Wang Y, Szretter KJ, Vermi W, Gilfillan S, Rossini C, Cella M, Barrow AD, Diamond MS, Colonna M. IL-34 is a tissue-restricted ligand of CSF1R required for the development of Langerhans cells and microglia. Nat Immunol. 2012; 13:753–760. [PubMed: 22729249]

Wegiel J, Wisniewski HM, Dziewiatkowski J, Tarnawski M, Kozielski R, Trenkner E, Wiktor-Jedrzejczak W. Reduced number and altered morphology of microglial cells in colony stimulating factor-1-deficient osteopetrotic op/op mice. Brain Res. 1998; 804:135–139. [PubMed: 9729335]

Wohl SG, Schmeer CW, Friese T, Witte OW, Isenmann S. In situ dividing and phagocytosing retinal microglia express nestin, vimentin, and NG2 in vivo. PLoS One. 2011; 6:e22408. [PubMed: 21850226]

Yokoyama A, Yang L, Itoh S, Mori K, Tanaka J. Microglia, a potential source of neurons, astrocytes, and oligodendrocytes. Glia. 2004; 45:96–104. [PubMed: 14648550]

Zhan Y, Paolicelli RC, Sforazzini F, Weinhard L, Bolasco G, Pagani F, Vyssotski AL, Bifone A, Gozzi A, Ragozzino D, et al. Deficient neuron-microglia signaling results in impaired functional brain connectivity and social behavior. Nat Neurosci. 2014

Zhang C, Ibrahim PN, Zhang J, Burton EA, Habets G, Zhang Y, Powell B, West BL, Matusow B, Tsang G, et al. Design and pharmacology of a highly specific dual FMS and KIT kinase inhibitor. Proc Natl Acad Sci U S A. 2013; 110:5689–5694. [PubMed: 23493555]

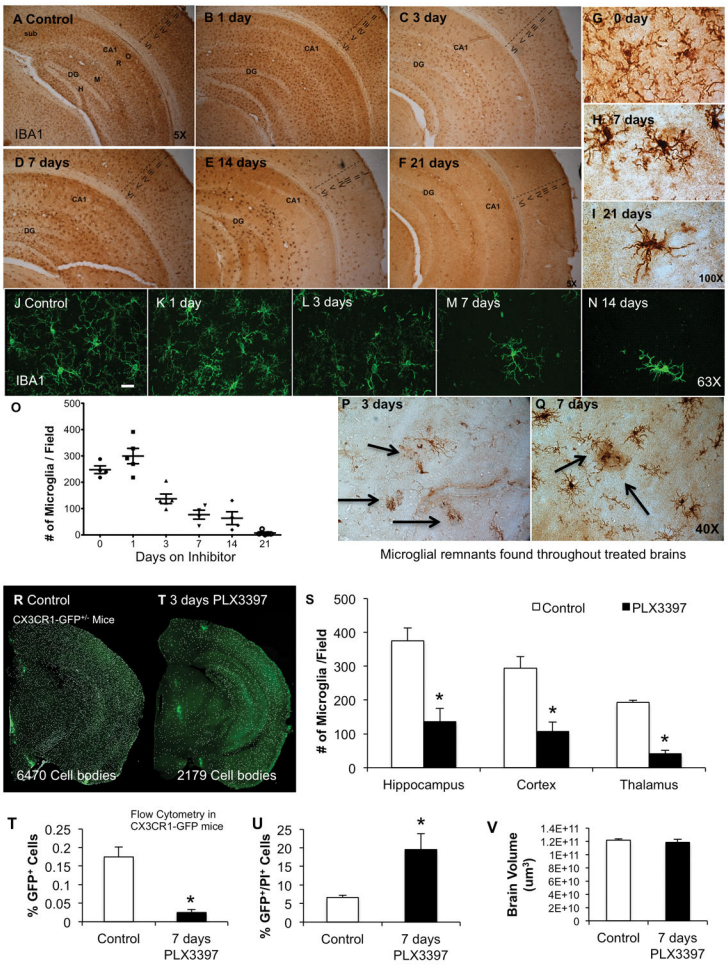

Figure 1. CSF1R inhibition eliminates microglia from the adult brain

12 month-old wild-type mice (C57BL/6/129 mix; n = 4–5 per group) were treated with PLX3397 (290 mg/kg chow) for 0, 1, 3, 7, 14, or 21 days. A–F) Immunostaining for IBA1 shows robust decreases in microglial numbers, with no detectable microglia present after 21 days of treatment. G–I) IBA1 immunostaining shows changes in microglia morphology during treatment, with representative microglia shown from control, 7-, and 21- days treated mice, imaged from between the blades of the dentate gyrus. J–N) Representative IBA1 immunofluorescent staining from the hippocampal region showing 63XZ-stacks of microglia during treatment. Scale bar represents 20 μM. O) Quantification of number of $IBA1^+$ cell bodies from a 10X field of view from the hippocampal regions as a function of time. Statistical analyses were performed via one-way ANOVA indicating $p < 0.0001$ for CA1, CA3, and subiculum, comparing all timepoints, shown as an average for all 3 regions. P, Q) $IBA1^+$ cell debris and non-intact cell parts were observed throughout the brains of mice treated with CSF1R inhibitors. Arrows indicate these microglial remnants alongside intact microglia. R–S) 2 month-old CX3CR1-$GFP^{+/-}$ mice were treated with PLX3397 or vehicle for 3 days (n = 3 per group). Brains were sectioned and the number of GFP^+ cell bodies counted from a 10X field of view of the hippocampus, cortex, and thalamus. Each white dot represents a GFP^+ cell body. T) 2 month-old CX3CR1-$GFP^{+/-}$ mice were treated

with PLX3397 for 7 days or vehicle (n = 3 per group). Brains were then extracted, dissociated into a single cell suspension, and then incubated with PI. Flow cytometry was then performed revealing >90% reduction in the number of GFP^+ cells with treatment compared to vehicle treated. U) The fraction of GFP^+ cells that were undergoing cell death, as shown by incorporation of PI, was significantly higher with PLX3397 treatment than vehicle, consistent with microglial cell death with CSF1R inhibition. V) Total brain volumes were measured via Cavalieri stereology in 2 month-old wild-type mice treated with PLX3397 or vehicle for 7 days (n = 4 per group). No significant differences were seen. * indicates significance ($p < 0.05$) by unpaired students T-test. Erorr bars indicate SEM. CA, cornusammonis; DG, dentate gyrus; O, stratum oriens; R, stratum; M, molecular layer dentate gyrus; H, hilus.

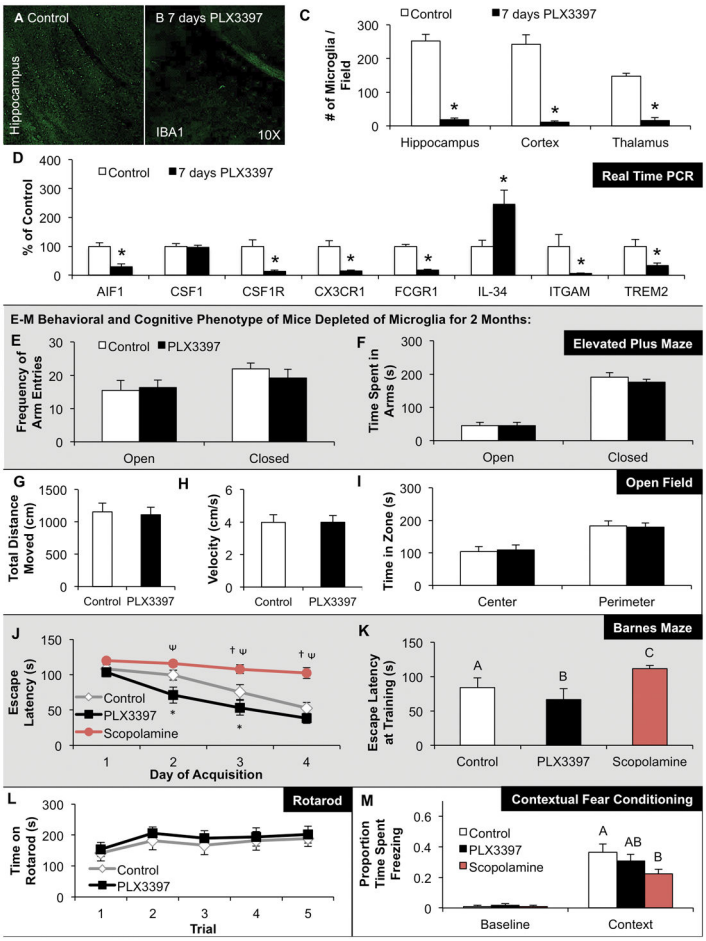

Figure 2. CSF1R inhibition reduces microglial markers and numbers, but does not affect brain volume, cognition, or motor function

A–D) 2 month-old wild-type mice were treated with PLX3397 for 7 days or vehicle (n = 4 per group). Representative images from brain sections stained with anti-IBA1 from the hippocampal region of control (A) and PLX3397 (B) treated mice. C) Quantification of the number of IBA1^{+} cell bodies in a 10X field of view from the hippocampus, cortex, and thalamus shows >90% elimination of microglia with 7 days PLX3397 treatment. D) Real Time PCR of mRNA extracted from half brains for microglial markers shows robust reductions in *AIF1*, *CSF1R*, *CX3CR1*, *FCGR1*, *ITGAM*, and *TREM2*. E–M) 2 month-old wild-type mice were treated for 2 months with PLX3397 or vehicle to deplete microglia from the CNS (n = 10 per group). E, F) Elevated plus maze showed no differences in the frequency of arm entries or time spent in the open or closed arms in microglia-depleted mice versus controls. G–I) Open field analysis showed no differences in the average total distance moved (G), the average velocity (H), or the relative amount of time spent at the edge of the arena versus the center (I) with microglial elimination. Combined, these two tasks demonstrate that mice depleted of microglia do not show increased anxiety. J, K) Microglia-depleted mice showed reduced escape latencies in the Barnes maze on days 2 and 3 of training compared to controls, as well as a lower average escape latency for all training sessions. Mice administered scopolamine (a cholinergic antagonist that causes memory

deficits) performed more poorly than both controls and PLX3397-treated mice. L) Accelerating rotarod showed no changes in mice depleted of microglia. M) As expected, animals treated with scopolamine had reduced memory in a contextual fear conditioning paradigm, but there were no differences in time spent freezing for controls or microglia-depleted mice. * indicates significance ($p < 0.05$) by unpaired students T-test, while same capital letters above conditions indicates no significant difference. For comparisons in (J): *$p < 0.05$ = CON vs. PLX; $^{\dagger}p < 0.05$ = CON + Scopolamine; $p < 0.05$ = PLX vs. CON + Scopolamine.

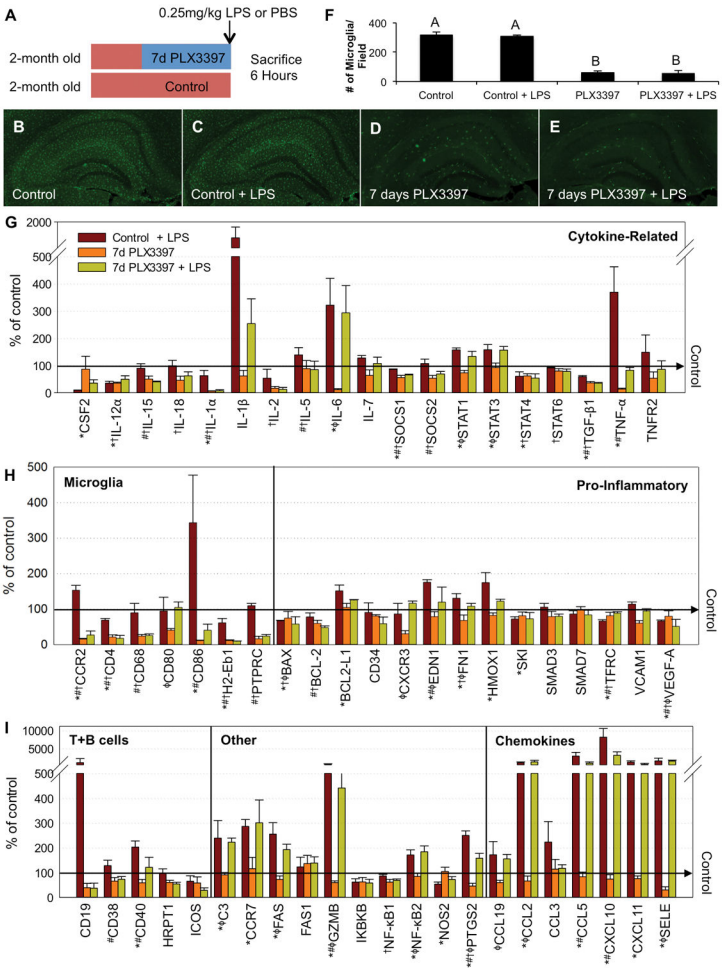

Figure 3. LPS challenge in microglia deficient brains

A) Schematic of the experimental design: 2 month-old C57BL/6 mice were fed either PLX3397 or control chow for 7 days. On day 7, mice were injected (IP) with either LPS (0.25 mg/kg) or PBS (n = 4 per group). Mice were euthanized 6 hours post-injection. B–E) Immunostaining for IBA1 shows robust decreases in microglial numbers for both PLX3397 and PLX3397 + LPS, which was confirmed by microglial counts (F). G–I) The relative mRNA expression of the microglia-devoid brain in response to LPS for a variety of inflammatory gene markers. Significance is dictated by the following symbols: Control vs. Control + LPS*; Control vs. PLX3397†; Control + LPS vs. PLX3397 + LPS$^{\#}$; PLX3397 vs. PLX3397 + LPS (all comparisons, $p < 0.05$). Full p-values can be found in supplemental Table 1. Erorr bars indicate SEM.

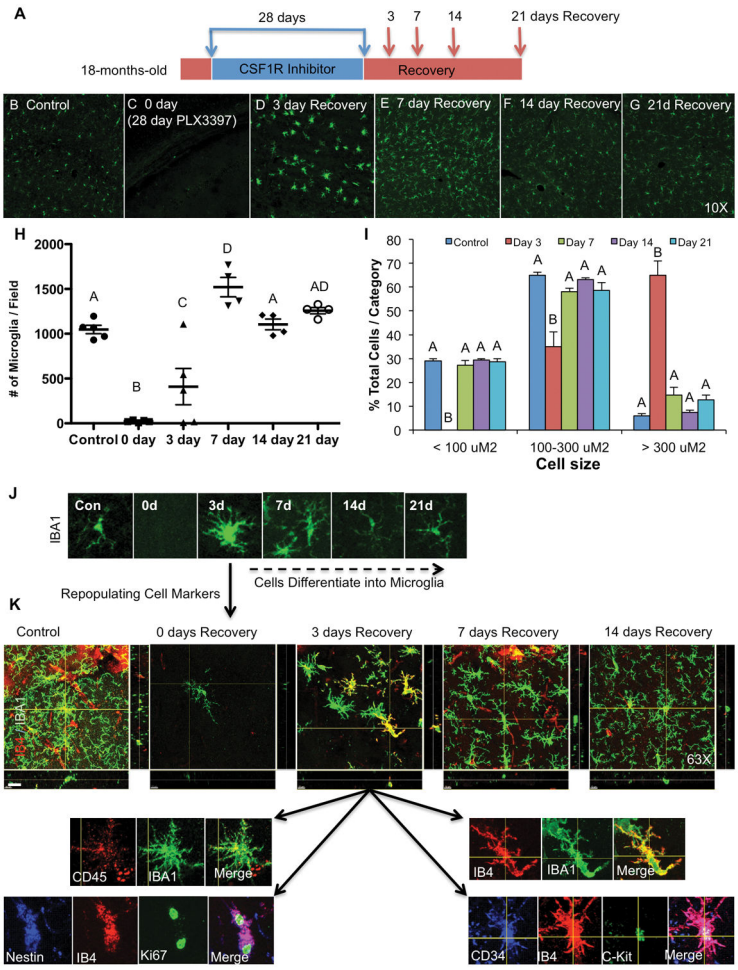

Figure 4. Rapid repopulation of the microglia-depleted brain with new cells that differentiate into microglia

A) To explore microglia homeostasis in the adult brain, 18 month-old wild-type mice were treated with PLX3397 for 28 days to deplete microglia. The inhibitor was withdrawn and groups of mice sacrificed immediately and at 3, 7, 14, and 21 days later (n = 4–5 per group). B–G) IBA1 immunostaining revealed microglia throughout the untreated (control) brains (B) and elimination of microglia in mice treated with PLX3397 (C). New IBA1$^+$ cells appeared throughout the CNS at the 3-day recovery timepoint with very different morphologies to control resident microglia (D). Cell numbers increased by the 7-day recovery timepoint and the morphology of the cells begin to resemble a more ramified state (E). By 14 (F) and 21 (G) days of recovery, the IBA1$^+$ cells resemble ramified microglia and have fully repopulated the entire CNS. H) Quantification of the number of IBA1$^+$ cells in the hippocampal field. I) Analysis of cell body size shows that IBA1$^+$ cells at the 3-day recovery timepoint are much larger than resident microglia. The size of these cells then normalizes over the following recovery timepoints. J) Representative IBA1$^+$ cells from each of the groups, showing the changes in cell morphology and size that occur during repopulation. K) Cells at the 3-day recovery timepoint express a number of unique markers, including CD45, nestin, Ki67, CD34, and c-kit. They also show high immunoreactivity to

the IB4 lectin. Notably, $IBA1^+$ cells in control brains and surviving $IBA1^+$ cells in the 0-day recovery group are negative for all these markers. Likewise cells at the 7-, 14-, and 21-day recovery timepoints are also negative for all these markers, highlighting that the initial repopulating cells have a unique morphology and phenotype. Same capital letters above conditions indicates no significant difference ($p>0.05$) via one-way ANOVA with post-hoc Newman-Keuls Multiple Comparison Test. Error bars indicate SEM. Scale bars represents 20 μM.

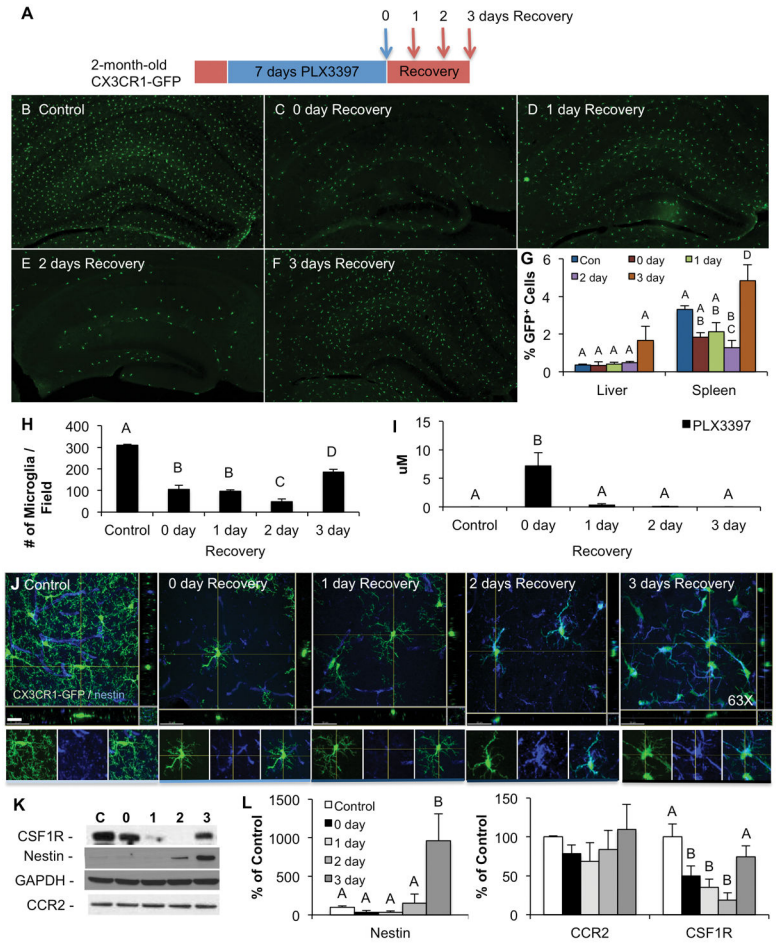

Figure 5. Microglial repopulation occurs between 48 and 72 hours after CSF1R inhibitor withdrawal

A) To investigate early repopulation events, 2 month-old CX3CR1-GFP$^{+/-}$ mice were treated with PLX3397 for 7 days. The inhibitor was then withdrawn and groups of mice sacrificed 1, 2, and 3 days later (n = 4 per group). B–F) Representative sections shown from the hippocampus of each of these groups, in which microglia express GFP. G) Flow cytometry of GFP+ cells from the liver and spleen of these animals. H) Quantification of whole brain sections for microglial numbers shows a reduction of ~70% with 7 days PLX3397 treatment. Microglial numbers continue to decline for 2 days after inhibitor withdrawal, but rapidly recover between days 2 and 3, highlighting a crucial time period in repopulation. I) Brain levels of PLX3397 show rapid clearance of the drug from the CNS. J) GFP^{+} cells strongly express nestin at the 2- and 3-day recovery timepoints. 63X Z-stacks obtained by confocal microscopy and maximal projections are shown. Scale bar represents 20 μM. Separate channels and merge are shown for each of the timepoints in the panels below. K) Western blots of whole brain homogenates show significant increases in nestin and CSF1R with repopulation, but no changes in CCR2. L) Quantification of K) normalized to GAPDH as a loading control. Same capital letters above conditions indicates no significance ($p>0.05$) via one-way ANOVA with post-hoc Newman-Keuls Multiple Comparison Test. Error bars indicate SEM.

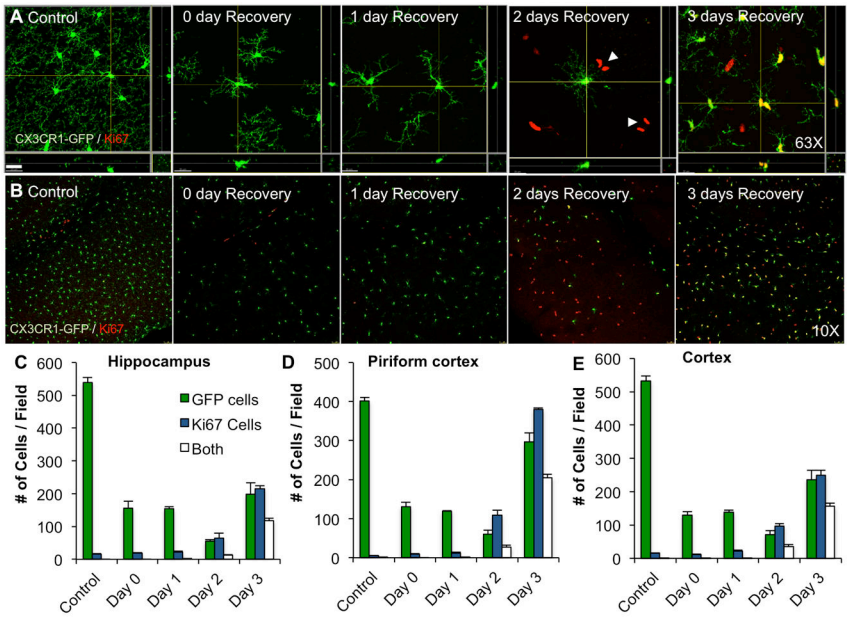

Figure 6. Microglial repopulation is preceded by proliferation of a non-microglial cell type throughout the CNS

Using the same experimental groups as shown in Figure 5, A) repopulating brains were stained for the cell proliferation marker Ki67. Few $Ki67^+$ cells were seen in control, 0-, or 1-day recovery groups. A fraction of the GFP^+ cells expresses Ki67 at the 2-day recovery timepoint and a majority of the GFP^+ cells express Ki67 at the 3-day recovery timepoint. Of note, $Ki67^+/GFP^-$ cells appeared throughout the CNS at 2 days of recovery, usually with two nuclei adjacent to one another, suggesting a recent cell division (highlighted by arrows). Far fewer $Ki67^+/GFP^-$ cells were seen at the 3-day recovery timepoint. 63X Z-stacks obtained by confocal microscopy and maximal projections are shown. Scale bar represents 20 μM. B) Images of $Ki67^+$ and GFP^+ cells from the cortex are shown to illustrate the number of proliferating, but GFP negative, cells that appear at the 2-day recovery timepoint, which is quantified in (C) for the hippocampal region, (D) for the piriform cortex, and (E) for the cortex. Same capital letters above conditions indicates no significant difference ($p>0.05$) via one-way ANOVA with post-hoc Newman-Keuls Multiple Comparison Test. Error bars indicate SEM.

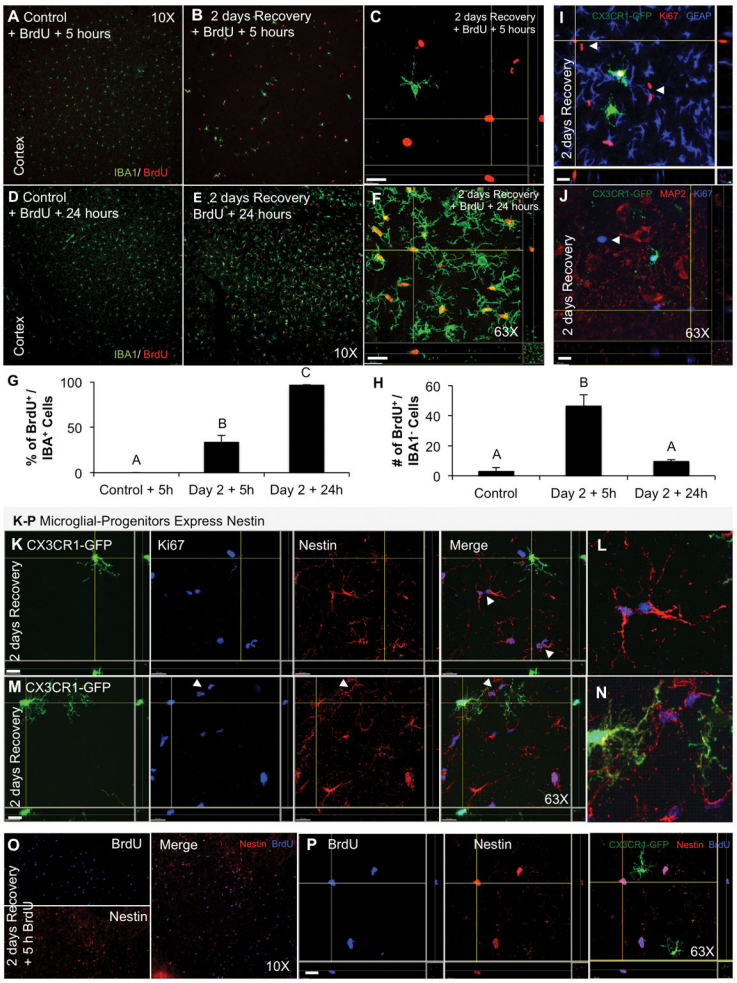

Figure 7. Fate mapping reveals a nestin-expressing microglia progenitor cell that becomes the repopulating microglia

A–C) To determine if the non-microglial Ki67^{+} proliferating cells were becoming microglia, 2 month-old wild-type mice were treated with PLX3397 or vehicle to deplete microglia. The inhibitor was withdrawn and BrdU administered 2 days later to label proliferating cells (n = 3–4 per group). Mice were sacrificed 5 or 24 hours later (n = 4 per group). Representative images of the cortical region are shown for controls (A) and the 2-day recovery group (B) for IBA1 and anti-BrdU at 5 hours following BrdU administration. 63X maximal projection Z-stacks are shown for the 2-day recovery group + 5 hours BrdU (C), revealing that the vast majority of BrdU-incorporated cells are not microglia. D–F) Representative images of the cortical region are shown for controls (D) and the 2-day recovery group (E) for IBA1 and anti-BrdU at 24 hours following BrdU administration. 63X maximal projection Z-stacks are shown for the 2-day recovery group at 24 hours following BrdU administration (F), revealing that the vast majority of BrdU-incorporated cells are now microglia. G) Quantification of A–F shows that only 30% of BrdU-incorporated cells are microglia after 5 hours, but 96% become microglia after 24 hours. H) Quantification of the total amount of BrdU^{+}/non-microglial cells per field of view shows that most of these cells have differentiated into microglia within 24 hours. K, M) CX3CR1-GFP$^{+/-}$ mice were treated for

7 days with PLX3397, and 2 days after inhibitor withdrawal, $Ki67^{+}/GFP^{-}/nestin^{+}$ cells are induced throughout the CNS (highlighted with white arrow heads; two different fields of view are shown, with a zoom image of the nestin expressing cells shown in L and N). In addition, co-stains with Ki67 show that the repopulating cells do not express GFAP (I) or MAP2 (J). O, P) BrdU-incorporated cells in the 2-day recovery brains (sections obtained from (B) above), also express nestin (microglia only shown in the 63X merge). Same capital letters above conditions indicates no significant difference ($p>0.05$) via one-way ANOVA with post-hoc Newman-Keuls Multiple Comparison Test. Error bars indicate SEM. Scale bars represents 20 μM.

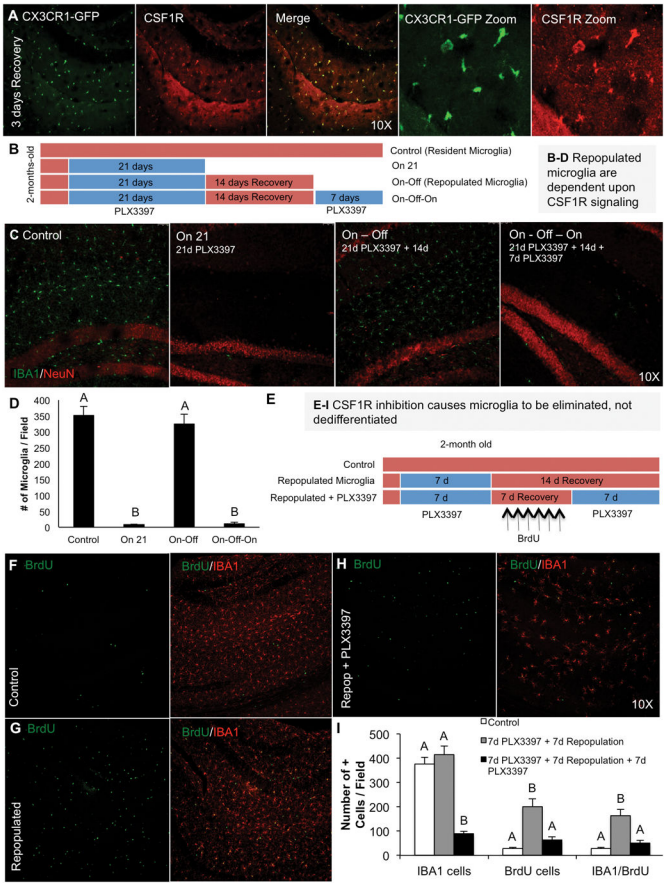

Figure 8. Microglia are eliminated with CSF1R inhibition and not dedifferentiated

A) Repopulating microglia express CSF1R – 3-day recovery timepoint shown. B) Schematic of the experimental design: 2 month-old mice were treated for 21 days with PLX3397 to deplete microglia (“on”). PLX3397 was then removed from the diet in a second group and repopulation allowed for 14 days (“on-off”). A final group was then treated for a second time with PLX3397 (“on-off-on”, n = 4–5 per group) to determine if repopulated microglia were also eliminated with CSF1R inhibition. C) Representative sections from the hippocampal field for IBA1 and NeuN from each of the four groups. D) Quantification of IBA1 cells in matching full brain sections shows that repopulating microglia are also fully dependent upon CSF1R signaling. E) Schematic of the experimental design: 2 month-old wild-type mice were treated with PLX3397 for 7 days to deplete microglia. PLX3397 was removed to allow microglia to repopulate and BrdU was administered daily to tag these new cells. 7 days later, PLX3397 was re-administered to BrdU-tagged microglia containing mice. F–H) Representative stainings from the hippocampal region for BrdU and IBA1 show that repopulating microglia incorporate BrdU (G) and that PLX3397 treatment eliminates both IBA1 cells and BrdU-incorporated cells (H). I) Quantification of (F–H). Same capital letters above conditions indicates no significant differences ($p>0.05$) via one-way ANOVA. Error bars indicate SEM.